Academic Science Journal

Changes Detection of Land Surface Temperature over Southern Of Iraq during Period (1990 – 2022) Using Landsat Data

Marwa K. Tawfik* and Alaa M. Al-Lami

Department of Atmospheric Sciences, College of Science, Mustansiriyah University

marwa.khalid@uomustansiriyah.edu.iq

Received: 20 May 2024 **Accepted: 18 August 2024**

Published: 30 April 2025

DOI: https://dx.doi.org/10.24237/ASJ.03.02.886B

Abstract

Land surface temperature (LST) is one of the important essential climate variables for climate change studies. It helps in giving valuable information to characterize land surface states and land-atmosphere exchange. This study presents LST's spatial and temporal patterns in Basra, Thi-Qar, and Maysan, which are three provinces in southern. Dependent on Landsat 5TM and 8OLI imagery in 1990, 2013, and 2022. The LST was estimated in July (representative for summer) and December (representative for winter) of each year. Using ArcGIS 10.8, supervised classification was made to quantify the spectral pixels of the LST into different ranges. The results showed for July that there was an apparent increase in temperatures in the study area, especially in Basra and Zubair districts in Basra province. This study investigates most of the areas of Thi-Qar, such as Shatra, and some of the Maysan areas, as they are considered humid areas due to the existing marshes. The LST values ranged from 23-58 °C for Basra, 21-55 °C for Thi-Qar, and 23-57 °C for Maysan. In December, the values ranged 3-24 °C for Basra, 3-28 °C for Thi-Qar, and 4-23 °C for Maysan. The results also showed that LST was mainly related to changes in land surface cover. Generally, in the whole area of the three provinces, there was a

significant increase in LST from 1990 to 2022, especially for the thermal range (41-51 C°) in summer. Similarly, in December, there was a continuous increase in LST of 16-22 C°, which was evident with more intensity in 2022 in Basra and Maysan.

Keywords: Land surface temperature, Urban areas, Landsat, Remote sensing; GIS.

Introduction

Land surface temperature (LST) is considered one of the main parameters in studying the transformation of urban surfaces such as natural land cover (e.g., vegetation, water bodies, bare ground, parks, trees, etc.) into impervious surfaces such as roads, buildings, and other urban features, which have a significant impact on the urban environment[1][2][3]. The urban environment can absorb most of the incoming radiation, and as a result, the air in contact with the Earth's surface becomes warmer than the surrounding rural areas. The difference in land absorption of sunlight between urban areas and rural areas has led to a gives rise to a phenomenon known as urban surface heat island (SUHI)[4][5]. LST is temperature of the Earth's crust, while its measurement can provide important data on energy balance, physical surface temperature, microclimate, and human activities, so it plays a crucial role in ecosystems, environmental protection, and ecology[6][7]. Human activities are recognized to be the primary cause of this phenomenon and the increase in surface temperature [8]. Many studies addressed LST due to its usefulness in many fields such as water cycle, urbanization change, climate change, evaporation, and monitoring of green surfaces and the environment[9][10]. Thermal remote sensing stands out among several available methods that allow the spatial estimation of LST in large urban areas using satellite imagery with infrared bands. Based on medium-resolution Landsat images, many studies have been estimated to capture the LST scene[11][12]. Many studies used LST information to calculate relationship with LULC changes as shown. Zhang et al.,(2019) Investigated The effects of land use and cover on the thermal properties of urban land were discussed from three angles: the relationship of surface temperature with land cover and population density; Seasonal changes in temperatures within cities; The intensification of the urban heat island effect due to the growth of built-up land in urban areas.be used Land surface information, derived from satellite imagery, and complementary information such as demographics [13]. Tran et al.,2017, This study examined the relationship between LULC change and UHI impacts. The results provided an effective methodology for characterizing universal health coverage and have significant implications for policy makers and communities by providing a scientific basis for sustainable urban planning and management in the city of Hanoi [14], Alahmad et al. (2020) conducted a study about LST in Kuwait. Urbanization has replaced naturally occurring desert regions and open dirt with artificially constructed infrastructure and surfaces. Satellite data over the last 17 years indicates an urban cool island during the day and an urban heat island at night. This research can help with attempts to adapt to climate change, particularly in the area of urban planning [15]. Soydan (2020) The study presented the importance of vegetation cover on surface temperature through heat island analysis in Nigde, Turkey. The results indicated the mitigation of heat islands and temperature differences between cities and rural areas, which provides important insights into improving the management strategy of environments (urban and rural) [16]. Abulibdeh et al., 2021 . Researchers in the Arabian Gulf region conducted an examination of the heat island features of eight towns, which are located in dry and semi-arid environments. The findings demonstrated substantial variations in the features of heat islands among cities, which may be attributed to environmental conditions and human activities. This conclusion was drawn based on the study of remote sensing data and spatial analytic techniques. They proposed mitigating measures such as expanding the number of green areas and enhancing surface coverings. The study findings suggested enhancing architectural design and mitigating the impacts of urban heat islands[17]. Saraskanrood et al., 2023 in Iran. An investigation was conducted to analyze the influence of land use on surface temperatures using remote sensing data. The findings revealed a distinct thermal pattern in built-up regions as opposed to rural areas, suggesting that alterations in land use had an impact on surface temperatures. This study offers support in enhancing urban planning and facilitating adaptation to climate change [18]. in Iraq several studies have mapped LST, particularly in southern part such as Basra [19] and Babylon [2] using GIS techniques.

The study conducted by Salman and Al Razaq (2023) calculated LST values for two months in 2013 and 2021 (July and December). They discovered a stronger relationship between changes in urban land cover and LST. Knowledge of LST distributions in a particular location is very useful in the urban planning process and necessary for a sustainable urban environment. This current study aims to detect the change of the land surface temperature in two different contrasting seasons, summer and winter, in three years periods, 1990, 2013, and 2020, in three cities for southern Iraq, The study area is an important economic area, where most people work in agriculture, especially crops, grain production, and some common vegetables[20]. for using Landsat 5, 8 LST.

Material and methods

Study area and data

The study area is the southernmost part of Iraq, including three provinces: Basra, Thi-Qar, and Maysan (see Fig.1). It shares boundaries with Saudi Arabia, Kuwait, and Iran. The geographical properties of each province, such as latitude, longitude, mean elevation (m) above sea level, and areas, are reported in Table 1. The total area of this study covers 48983 km^2, which forms 11.2% of Iraq's area[21]. Within the study area, there are wetland areas called marshlands, which are primarily located on the floodplains of the two Mesopotamian Rivers (Euphrates and Tigris)[22].

They are joined at Al-Qurnah in Basra and empty the water into the sea. Much of the land is desert. The climate of the marshes region is described within the Iraqi alluvial plain, characterized by hot and humid summers and cold winters with rainfall. The temperature ranges between 35˚-50˚in the summer, and in January, it reaches 0°C In the winter, the northeastern winds prevail in the marshes, and in the summer, the northwest winds blow over the marshes [20][23][24]. While the average rainfall is less than 25 mm/year [25].

Academic Science Journal

Table 1: Geographical properties for three Iraqi provinces.

Province	Latitude (N)	Longitude (E)	Elevation (M)	Area (Km^2)	Total of The Area (%)
Basra	31° 16″	46° 34″	5	19070	4.35
Thi-Qar	30° 40″	46° 19″	13	13841	3.16
Maysan	31° 00″	46° 00″	12	16072	3.67

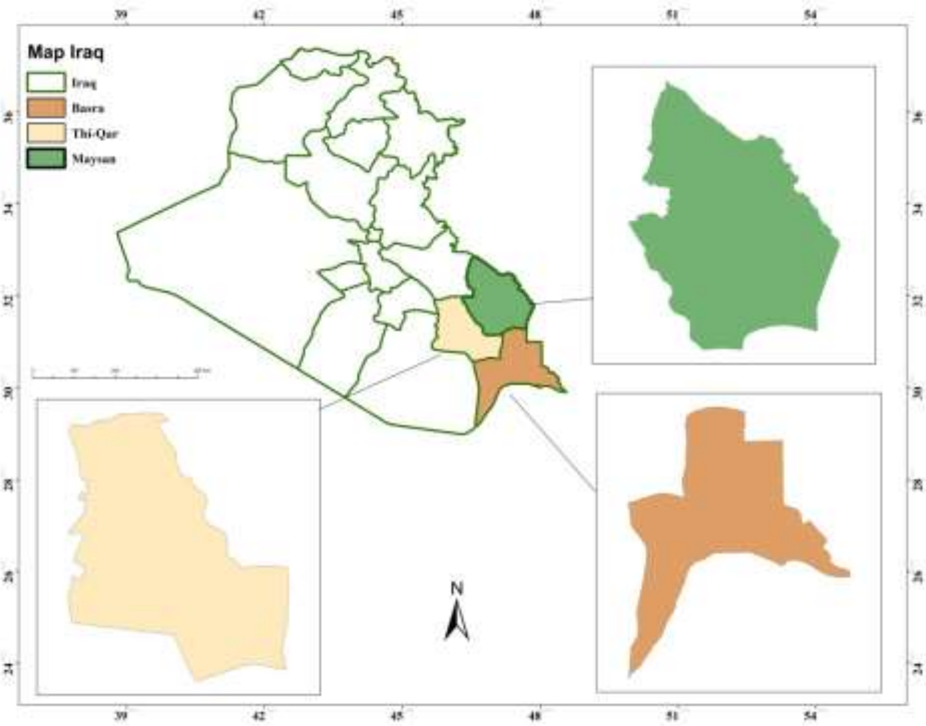

Figure 1: Study area of the southern region of Iraq comprised of Basra, Maysan, and Thi-Qar.

Methodology

The detection of LST for three southern provinces of Iraq was separately performed using remote sensing data from two Landsat satellite images 5 Thermal Mapper (TM) and 8 Operational Land Imager (OLI). The first Landsat 5 TM is dated in only two months July and December 1990 and the second Landsat 8 OLI is dated in the same months, but in two years 2013 and 2022. All of the images (total of 18 images) have cloud coverage of less than 10% and were acquired from the USGS portal *(www.earthexplorer.usgs.gov).* Also, Landsat 5 TM data include one thermal infrared band (band 6) with a resolution of 120 m and six multispectral bands with a spatial resolution of 30 m. Meanwhile, Landsat 8 OLI data used only band 10. The selected images were georeferenced using UTM zone 38 and WGS 84 projection system with path and row as shown in Table 2.

Table 2: The satellite information used for the study.

Governorate	Satellite	SENSOR	Path / row	Images	Time
Basra	**LANDSAT -5**	**TM**	**166/039**	**29 JULY 1990**	**23:04**
	LANDSAT -5	**TM**	**166/039**	**28 December 1990**	**17:37**
	LANDSAT -8	**OLI/TIRS**	**166/039**	**28 JULY 2013**	**07:24**
	LANDSAT -8	**OLI/TIRS**	**166/039**	**03 DECEMBER 2013**	**07:23**
	LANDSAT -8	**OLI/TIRS**	**166/039**	**21 JULY 2022**	**07:22**
	LANDSAT -8	**OLI/TIRS**	**166/039**	**20 DECEMBER 2022**	**07:22**
Maysan	**LANDSAT -5**	**TM**	**166/038**	**29 JULY 1990**	**23:19**
	LANDSAT -5	**TM**	**166/038**	**28 DECEMBER 1990**	**14:25**
	LANDSAT -8	**OLI/TIRS**	**166/038**	**28 JULY 2013**	**07:23**
	LANDSAT -8	**OLI/TIRS**	**166/038**	**03 DECEMBER 2013**	**07:23**
	LANDSAT -8	**OLI/TIRS**	**166/038**	**21 JULY 2022**	**07:21**
	LANDSAT -8	**OLI/TIRS**	**166/038**	**20 DECEMBER2022**	**07:22**
Thi-Qar	**LANDSAT -5**	**TM**	**167/038**	**04 JULY 1990**	**21:15**
	LANDSAT -5	**TM**	**167/038**	**27 DECEMBER 1990**	**15:05**
	LANDSAT -8	**OLI/TIRS**	**167/038**	**19 JULY 2013**	**07:29**
	LANDSAT -8	**OLI/TIRS**	**167/038**	**10 DECEMBER 2013**	**07:29**
	LANDSAT -8	**OLI/TIRS**	**167/038**	**28 JULY 2022**	**07:28**
	LANDSAT -8	**OLI/TIRS**	**167/038**	**19 DECEMBER 2022**	**07:28**

Land surface temperature

To produce digital LST maps, the infrared thermal band 6 (10.4-12. micron) from Landsat 5 for the sensor (TM) and band 10 from Landsat 8 for sensor (OLI/TIRS) were used. Using digital numbers (DN), the spectral radiance (L_λ) at top of the atmosphere expressed in unit W/m^2. was first calculated by the following equations (1) and (2) for Landsat 5 and Landsat 8 respectively [26]; [4]

$$L_\lambda = \left(\frac{L_{max\lambda} - L_{min\lambda}}{QCal_{max} - QCal_{min}}\right) * (QCal - QCal_{min}) + L_{min\lambda} \quad (1)$$

$$L_\lambda = M_L * QCal + A_L \quad (2)$$

where QCal is the quantized calibrated pixel value in DN, $QCal_{max}$ and $QCal_{min}$ are maximum and minimum quantized calibrated pixel values in DN, respectively, $L_{max\lambda}$ is the maximum radiance of band 6, $L_{min\lambda}$ is the minimum radiance of band 6, M_L is the radiance multiplicative factor of the band that is located in metadata file of the Landsat images (=3.342 x10^{-4} W/m^2.sr.μm); Q_{cal} is the DN of the bands (0-255), and A_L is the additive radiance scaling factor for the TIRS bands. Secondly, L_λ was converted to brightness temperature (T) in °C using the conversion formula below

$$T = K_2 * \left[\ln\left(\frac{K_1}{L_\lambda} + 1\right)\right]^{-1} \tag{3}$$

Where, K1 & K2 are the calibration constants of thermal bands. The third step includes calculating the emissivity (ε) of the earth's surface using the equation

$$\varepsilon = 0.004 * Pv + 0.986 \tag{4}$$

Where Pv is the proportional vegetation derived from the Normalized Difference Vegetation Index (NDVI) as written

$$Pv = \left[\frac{(NDVI - NDVI_{min})}{(NDVI_{max} - NDVI_{min})}\right]^2 \tag{5}$$

where NDVImin and NDVImax are the maximum and minimum NDVI. Finally, from equations (3) and (4), LST was computed by the equation

$$LST = \frac{T}{1+\left(\frac{\lambda * T}{\rho}\right) * \ln\varepsilon} - 273.15 \tag{6}$$

Where λ is the average wavelength of the emitted radiation (=11.457 and 10.8 μm for Landsats 5 and 8, respectively) and ρ the constant value (=1.438x10^{-34} J.s). Fig. 2 shows a diagram of the methodology used in the present study. In order to classify LST values into several categories, the geographic information system software ArcGIS 10.8 was used to achieve the supervised classification process by means of the maximum likelihood algorithm. This requires many samples for training for every class of LST images. The number of 50 samples were selected for every class of different surfaces such as water, plants, and barren. Lastly, this work has utilized using Google Earth for the field survey as reference data.

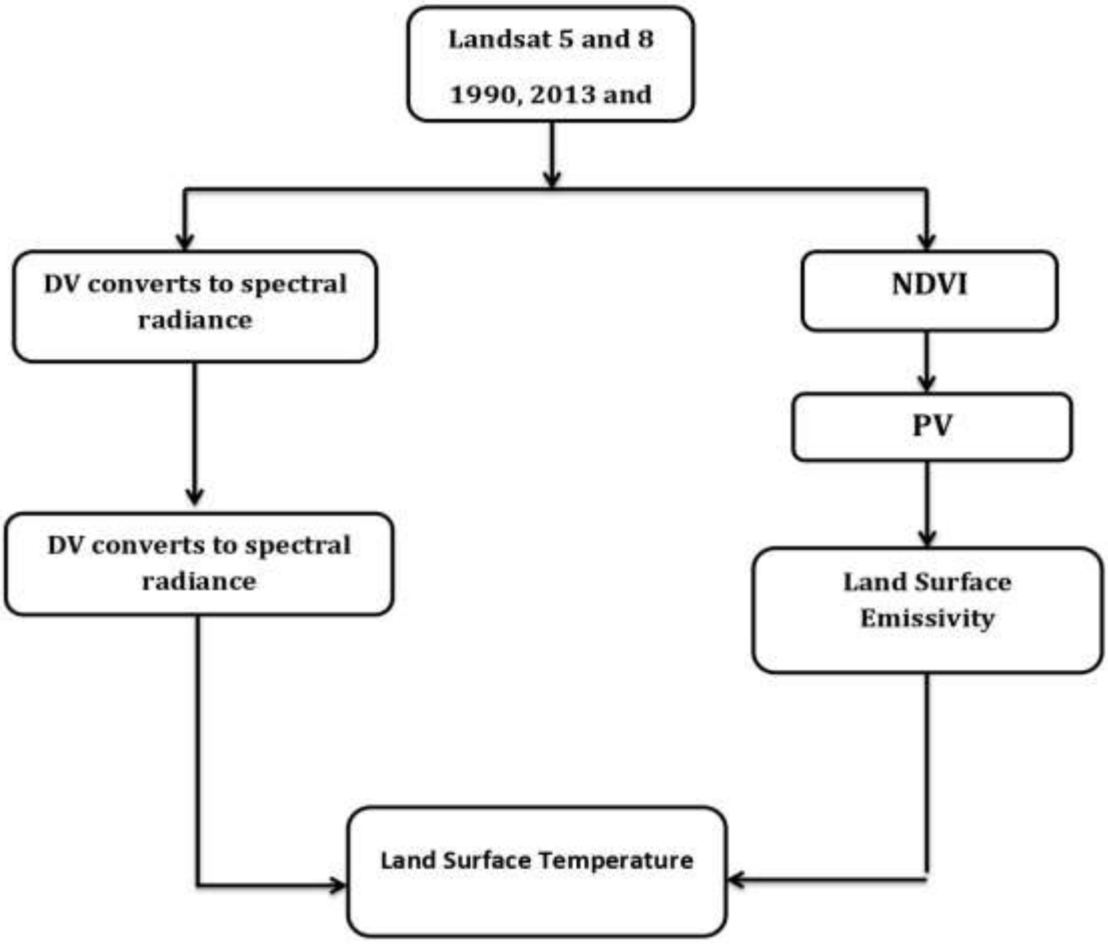

Figure 2: Flowchart showing the methodology.

Results and Discussion

LST distribution

Based on Eqs.(2), (3),and(5), the Landsat thermal images in this study were extracted for three cities, Basra, Thi-Qar, and Maysan at two different seasons summer and winter represented by July and December for three years 1990, 2013 and 2022.The spatial distributions of surface temperature through the research areas for two seasons of all years are presented in Figs. (3-5). In general, the minimum - maximum values of LST for July were 23.7 - 58.9 C^{o} for Basra, 20.7-

53.3 C° for Thi-Qar, and 23.8 - 56.6 C° for Maysan. For both July and December, values of LST were mostly increasing from 1990 through 2013 to 2022 for the whole area. This increasing in LST may belong to removing large areas of vegetation cover and also for urbanization which enhancing the effect of heat is land See (Fig. 3 , 4). However, the changing in LST for Maysan province for July for the three years were small and insignificant See (Fig. 5). This may belongs to the effect of existence of the two marshes which help in maintaining and conservation of LST values [27][20] .Table 3 lists the ranges of LST values for spatial thermal intervals.

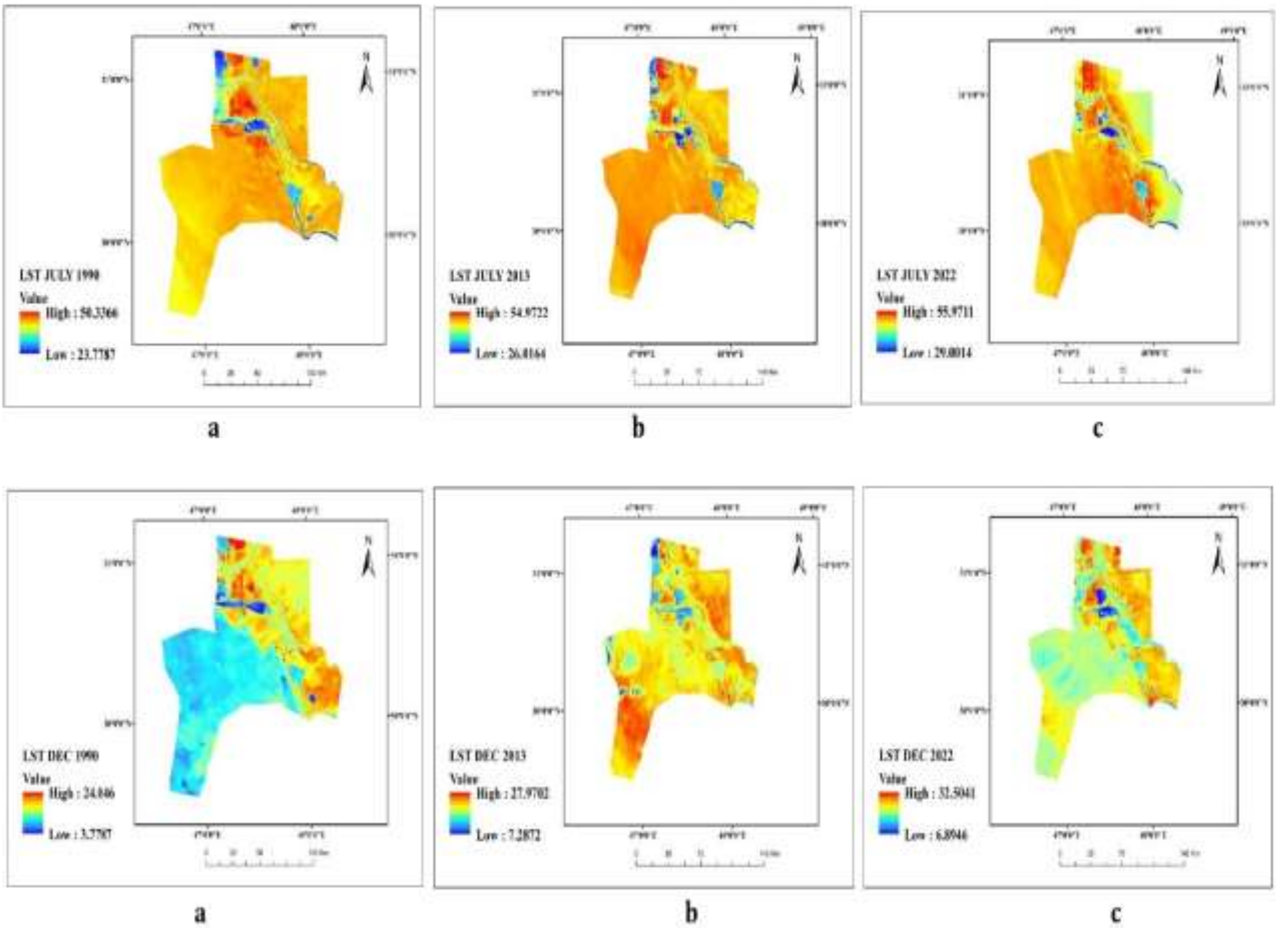

Figure 3: Spatial distribution of LST in Basra for years:(a) 1990, (b) 2013 and (c) 2022 : (upper: July and lower: December).

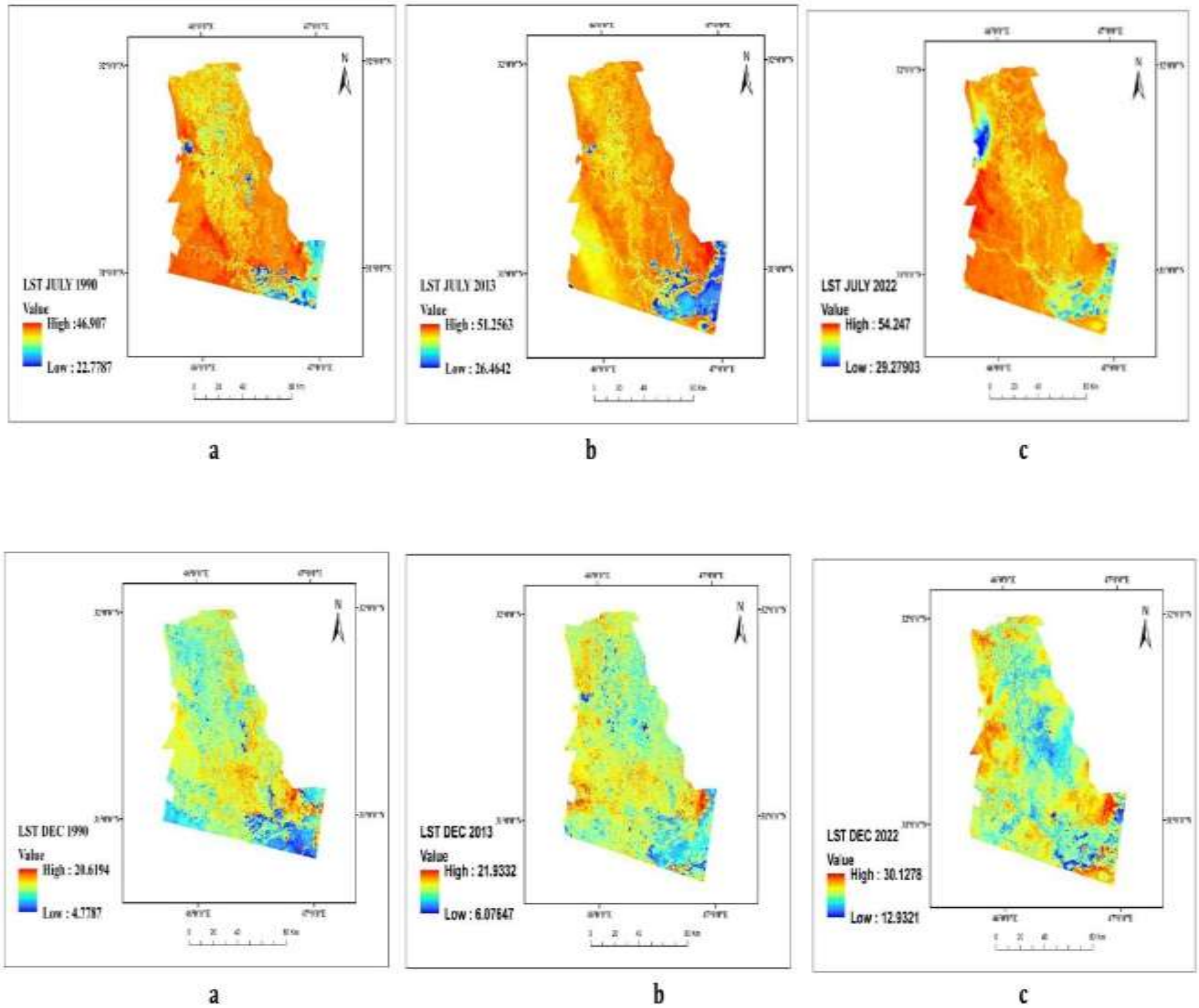

Figure 5: Spatial distribution of LST in Maysan for years: :(a) 1990, (b) 2013 and (c) 2022: (upper: July and lower: December)

Table 3: Interval and range values of LST for July and December in the three southern provinces of Iraq.

Month	Basra		Thi-Qar		Maysan	
	Interval	**Range**	**Interval**	**Range**	**Interval**	**Range**
July	**23 - 58**	**35**	**21-55**	**34**	**23-57**	**34**
December	**3-24**	**21**	**3-28**	**25**	**4-23**	**19**

Academic Science Journal

The LST areas were divided into five subintervals according to the total area of each governorate, as shown in Table 3. he total extent of the LST was divided into five thermal periods for both months, as shown in Tables 4-6 for July and tables 7-9 for December, These tables were used then to calculate the areas in square kilometers for each year. Their proportions were then calculated according to the total individual area, using ArcGIS. In 1990, the LST of the thermal period (51- 58) was concentrated in the northern part of Basra, like the Qurna region, and some areas of the southwest, where oil fields are spread. In 2022, the maximum values of LST in Basra for July was extended to the southern parts such as the Basra and Zubair districts. This may due to the increased population, commercial and the Industrial activities. The thermal period (7.2-11.4) was the dominant one for the year 1990, especially in the southwest of Basra, and the LST rate increased in most areas of Basra in 2022 during the thermal period (15.6-19.8) by 10.8% for the regions Fig. 6, 7.

Table 4: Percentages of LST subintervals in Basra for July of 1990, 2013 and 2022.

LST	COLORS	1990	2013	2022
23 - 30		**1.364061**	**1.116792**	**0.145597**
30 - 37		**4.415441**	**4.025993**	**3.087032**
37 - 44		**11.218373**	**2.938094**	**9.448868**
44 - 51		**82.263568**	**77.715857**	**69.478878**
51 - 58		**0.738559**	**14.203265**	**17.839625**

Table 9: Percentages of LST subintervals in Maysan for December of 1990, 2013, and 2022.

LST	COLORS	1990	2013	2022
4 – 7.8		**2.282398**	**0.561349**	**0.000005**
7.8 – 11.6		**44.362886**	**3.776336**	**0.798391**
11.6 – 15.4		**47.507138**	**39.944296**	**57.40083**
15.4 – 19.2		**5.548639**	**53.99246**	**36.922632**
19.2 - 23		**0.298939**	**1.725559**	**4.878143**

Academic Science Journal

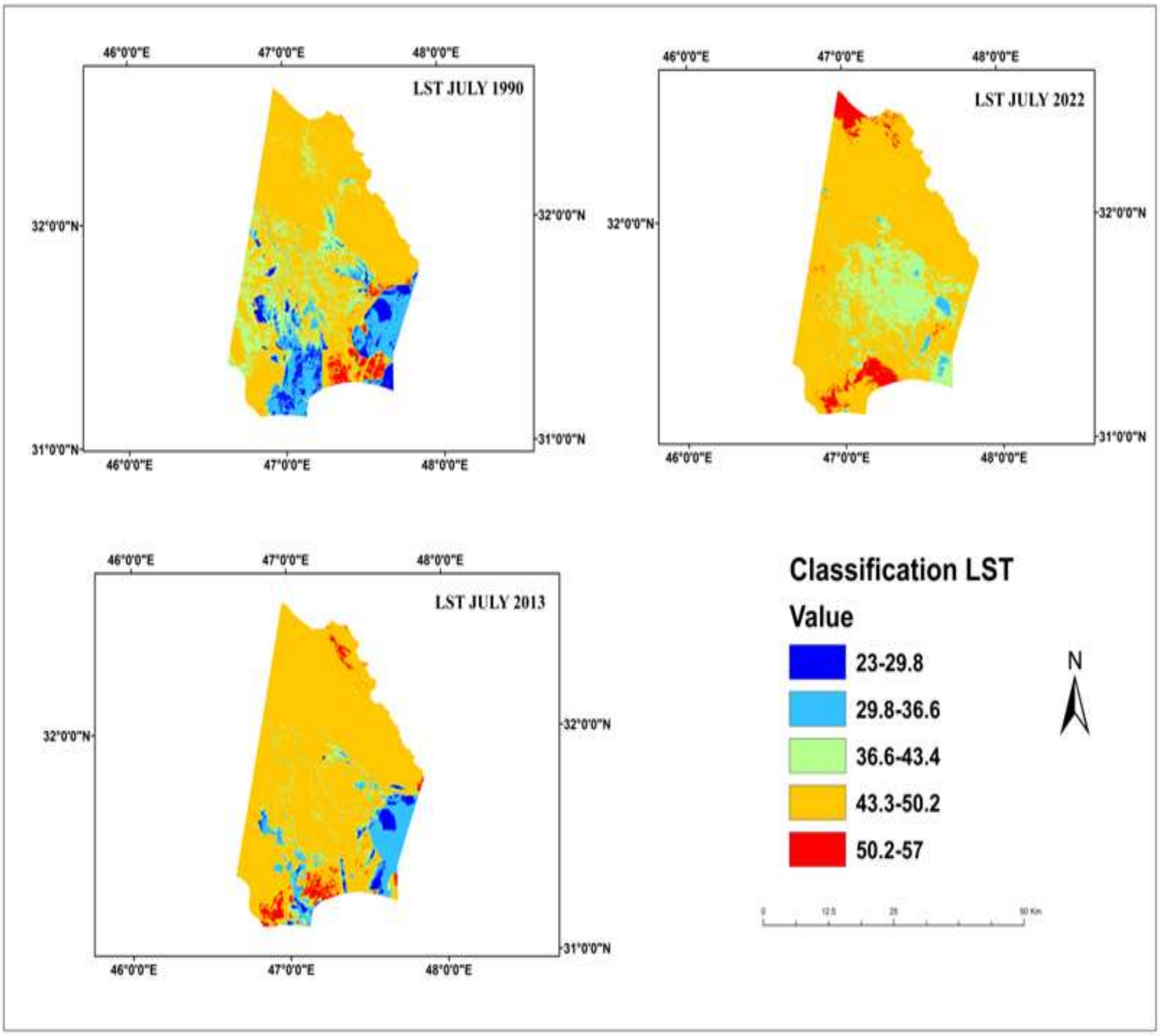

Figure 10: Spatial distribution of Supervised classification of LST in Maysan for years in ULY:1990, 2013,and 2022

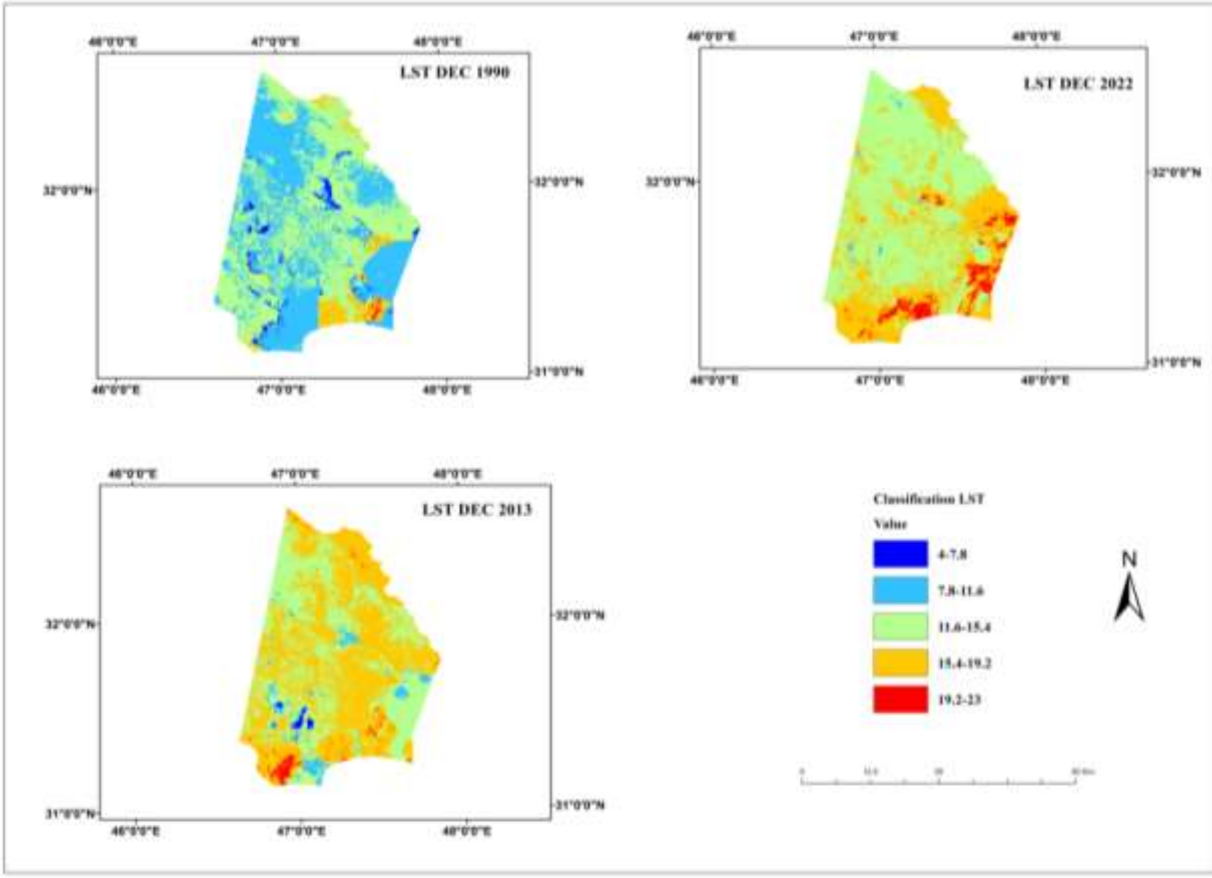

Figure 11: Spatial distribution of Supervised classification of LST in Thi-Qar for years in December: 1990, 2013, and 2022.

Conclusion

This study estimated the land surface temperature (LST) for the southern region of Iraq, including the provinces of Basra, Thi-Qar, and Maysan, during the summer and winter seasons for the years 1990, 2013, and 2022. We used satellite images from Landsat 5 TM and 8 OLI to calculate LST, which helps to observe the impacts of land use and land cover changes over these years. LST was computed using brightness temperature, NDVI, and land surface emissivity, and spatial maps were created to show LST distribution, classified into five thermal intervals. In summer (July), the highest average LSTs were 58°C in Basra, 55°C in Thi-Qar, and 57°C in Maysan. In winter (December), these averages were 24°C, 28°C, and 23°C, respectively. The lowest average LSTs in winter were 3°C in Basra and Thi-Qar, and 4°C in

Maysan. In summer, the lowest averages were 23°C in Basra and Maysan, and 21°C in Thi-Qar. In recent years, the areas with thermal ranges in the forties Celsius during summer have decreased compared to 1990 and 2013. In winter, the heat range between 9°C and 15°C was most significant in 1990 but decreased in 2013 and 2022.The NDVI index has an inverse relationship with LST, meaning higher NDVI values are associated with lower LSTs. Conversely, built-up areas, such as city centers, have a positive relationship with LST, leading to higher temperatures.

Acknowledgement

It is the authors' wish to express their gratitude and admiration for The Digital Elevation Satellite of the United States Geological Survey (USGS) for providing the required data for this study

Source of funding: This research was self-funded by the author, with no external financial support from any institution, organization, or commercial entity.

Conflict of interest: The author declares no conflict of interest. There are no personal, professional, or financial interests that could have influenced the outcomes of this study. The research is conducted independently, and the findings are solely based on the data analysis.

References

[1] A. AlKhudhairy, and Y. Kadhim, Analysis of the LST and Vegetation Indices relationship using Landsat-8 data in Duhok Governorate, Iraq, Al-Mustansiriyah J. Sci., 32, 6–12(2021), DOI(https://doi.org/10.23851/mjs.v32i4.1012)

[2] S. Alavipanah, M. Wegmann, S. Qureshi, Q. Weng, and T. Koellner, The role of vegetation in mitigating urban land surface temperatures: A case study of Munich, Germany during the warm season, Sustainability, 7(4), 4689–4706(2015) ,DOI(https://doi.org/10.3390/su7044689)

[3] H. J. Abdulla, Manifestations of Climate Change in Baghdad Area, Al-Mustansiriyah J. Sci., 30(4), 39–42(2019), DOI(http://doi.org/10.23851/mjs.v30i4.657)

[4] D. Hidalgo-García, and J. Arco-Díaz, Modeling the Surface Urban Heat Island (SUHI)

to study of its relationship with variations in the thermal field and with the indices of land use in the metropolitan area of Granada (Spain), Sustain. Cities Soc., 87, 104166, (2022), DOI(https://doi.org/10.1016/j.scs.2022.104166)

[5] F. Najafzadeh, A. Mohammadzadeh, A. Ghorbanian, and S. Jamali, Spatial and temporal analysis of surface urban heat island and thermal comfort using Landsat satellite images between 1989 and 2019: A case study in Tehran, Remote Sens., 13(21), 4469(2021), DOI(https://doi.org/10.3390/rs13214469)

[6] H. Govil, S. Guha, A. Dey, and N. Gill, Seasonal evaluation of downscaled land surface temperature: A case study in a humid tropical city, Heliyon, 5(6), (2019), DOI(https://doi.org/10.1016/j.heliyon.2019.e01923)

[7] Z. Li, Satellite remote sensing of global land surface temperature: Definition, methods, products, and applications, Rev. Geophys., 61(1), e2022RG000777(2023), DOI(https://doi.org/10.1029/2022RG000777)

[8] R. Yao, A robust method for filling the gaps in MODIS and VIIRS land surface temperature data, IEEE Trans. Geosci. Remote Sens., 59(12), 10738–10752(2021), DOI(https://doi.org/10.1109/TGRS.2021.3053284)

[9] A. Bendib, H. Dridi, and M. I. Kalla, Contribution of Landsat 8 data for the estimation of land surface temperature in Batna city, Eastern Algeria, Geocarto Int., 32(5), 503–513(2017), DOI(https://doi.org/10.1109/TGRS.2021.3053284)

[10] E. S. AL-Obaidey, The study of NDVI fluctuation in southern Iraq (Hor Ibn Najim) using remote sensing data, Al-Mustansiriyah J. Sci., 30(1), 1–6(2019), DOI(https://doi.org/10.1109/TGRS.2021.3053284)

[11] Z. L. Kozina, The influence of a special technique for developing coordination abilities on the level of technical preparedness and development of psycho-physiological functions of young volleyball players 14-16 years of age, (2018), DOI(http://dx.doi.org/10.7752/jpes.2018.03214)

[12] E. S. AL-Obaidey, Urbanization and its Effect on Land Surface Temperatures in Halabja City, (2021), DOI(https://doi.org/10.47577/technium.v3i10)

[13] Y. Zhang, and L. Sun, Spatial-temporal impacts of urban land use land cover on land surface temperature: Case studies of two Canadian urban areas, Int. J. Appl. earth Obs. Geoinf., 75, 171–181(2019), DOI(https://doi.org/10.1016/j.jag.2018.10.005)

[14] D. X. Tran, F. Pla, P. Latorre-Carmona, S. W. Myint, M. Caetano, and H. V Kieu, Characterizing the relationship between land use land cover change and land surface temperature, ISPRS J. Photogramm. Remote Sens., 124, 119–132(2017)

[15] B. Alahmad, L. P. Tomasso, A. Al-Hemoud, P. James, and P. Koutrakis, Spatial distribution of land surface temperatures in Kuwait: urban heat and cool islands, Int. J. Environ. Res. Public Health, 17(9), 2993(2020)

[16] O. Soydan, Effects of landscape composition and patterns on land surface temperature: Urban heat island case study for Nigde, Turkey, Urban Clim., 34, 100688(2020)

[17] A. Abulibdeh, Analysis of urban heat island characteristics and mitigation strategies for eight arid and semi-arid gulf region cities, Environ. Earth Sci., 80, 1–26(2021), DOI(https://doi.org/10.1007/s12665-021-09540-7)

[18] S. A. Saraskanrood, B. Asadi, and E. Ghale, Land surface temperature assessment in relation to land-use/land-cover (A case study: Isfahan City, Central Iran), Casp. J. Environ. Sci., 21(3), 725–735(2023), DOI(10.22124/CJES.2023.6959)

[19] A. F. Al-Yasiry, A. M. Al-Lami, and A. Al Maliki, Desertification Assessment for the Marshes Region Using Soil Quality Indicators, Southern Iraq, Iraqi Geol. J., 56(1), 259–272(2023), DOI(https://doi.org/10.46717/igj.56.1E.20ms-2023-5-30)

[20] B. M. Hashim, M. A. Sultan, M. N. Attyia, A. A. Al Maliki, and N. Al-Ansari, Change detection and impact of climate changes to Iraqi southern marshes using Landsat 2 Mss, Landsat 8 Oli and sentinel 2 Msi data and Gis applications, Appl. Sci., 9(10), 2016(2019), DOI(https://doi.org/10.3390/app9102016)

[21] I. Felix, A Multi-Layer Based Assessment of Wetland Changes in the Southern Iraqi Marshlands Using Remotely Sensed Data, Ike, F. Ottah, CR A Multi-Layer Based Assess. Wetl. Chang. South. Iraqi Marshlands Using Remote. Sensed Data. Int. J. Geosci., 10, 801–810(2019)

P-ISSN: 2958-4612
E-ISSN: 2959-5568

[22] F. House, Freedom in the World 2022-Iraq, Civil Lib., 13, 60(2022)

[23] K. Khosravi, Meteorological data mining and hybrid data-intelligence models for reference evaporation simulation: A case study in Iraq, Comput. Electron. Agric., 167, 105041(2019), DOI(https://doi.org/10.1016/j.compag.2019.105041)

[24] A. A. M. AF Al-Yasiry, AM Al-Lami, Desertification Assessment for the Marshes Region Using Soil Quality Indicators, Southern Iraq, Iraqi Geol. J., 56, 259–272(2023), DOI(https://doi.org/10.46717/igj.56.1E.20ms-2023-5-30)

[25] A. M. Al-Lami, Y. K. Al-Timimi, H. K. A. Al-Shamarti, Spatiotemporal analysis of some extreme rainfall indices over Iraq (1981–2017), Sci. Rev. Eng. Environ. Sci., 30(2), 221–235(2021), DOI(https://doi.org/10.22630/PNIKS.2021.30.2.19)

[26] A. A. Kafy, Remote sensing approach to simulate the land use/land cover and seasonal land surface temperature change using machine learning algorithms in a fastest-growing megacity of Bangladesh, Remote Sens. Appl. Soc. Environ., 21, 100463(2021)

[27] R. N. Al-Malikey, B. M. Hashim, and S. A. Abduljabbar, Using GIS to analyze some heavy metals concentrations in water of hammar, central and hawizeh marshes in southern Iraq, Al-Mustansiriyah J. Sci, 22(6), (2011)